

# FIELD EMITTER CURRENT CONDITIONING ON Nb SINGLE CRYSTALS WITH DIFFERENT ROUGHNESS DUE TO VARYING EP/BCP RATIO

S. Lagotzky, G. Müller, FB C Physics, University of Wuppertal, 42097, Germany  
P. Kneisel, TJNAF, Newport News, VA, USA

## Abstract

Systematic investigations of the influence of different EP to BCP polishing ratios ( $r_p = 0.15 - 5.80$ ) on the surface quality and the enhanced field emission (EFE) of dry ice cleaned Nb single crystals are reported. After removal of 138  $\mu\text{m}$  with  $r_p \leq 0.24$ , smooth surfaces with a roughness below 200 nm and few defects were obtained. EFE occurred at activation fields above 120 MV/m but the resulting onset fields  $E_{\text{on}}$  were often between 50 and 100 MV/m. Current conditioning up to 1  $\mu\text{A}$  reduced only the field enhancement factor but not the  $E_{\text{on}}$  values. Based on these results, the emitter number density of the actual ILC cavities is roughly estimated.

## INTRODUCTION

Particulate contaminations and surface irregularities are the main origin of enhanced field emission (EFE) of high-pressure-rinsed Nb surfaces [1]. Improved cleaning techniques like dry ice cleaning (DIC) and clean room assembly have led to a significant decrease of the number density  $N$  of particulate emitters [2]. However, the optimum choice of crystallinity and polishing of Nb is still under discussion [3]. For the future ILC cavities, large grain (LG) or even single crystal (SC) Nb with a combination of buffered chemical polishing (BCP) and electropolishing (EP) is considered [4]. Therefore, we have systematically investigated the EFE of DIC-SC Nb samples which got the same total polishing depth but a different EP/BCP ratio  $r_p$ . Since high peak power processing has been successfully used to remove EFE in SRF cavities [5], we have also started with the current conditioning of activated emitters up to 1  $\mu\text{A}$ .

## EXPERIMENTAL DETAILS

### Measurement techniques

For the systematic EFE and current conditioning measurements we have used a non-commercial field emission scanning microscope (FESM), which is in detail described elsewhere [6]. Non-destructive voltage scans  $V(x,y)$  for a limited EFE current ( $I = 1 \text{ nA}$ ) were performed in an area of 1  $\text{cm}^2$  with a resolution of 150  $\mu\text{m}$  to localize emitters and to determine their  $N$  as function of activation field  $E_{\text{act}}$  in reasonable steps (1 kV). Electric field maps up to 240 MV/m were derived for an average gap of  $\Delta z = 40 \mu\text{m}$  ( $E > 200 \text{ MV/m}$ ) or  $\Delta z = 50 \mu\text{m}$  ( $E \leq 200 \text{ MV/m}$ ).

The  $I(V)$  characteristics at all emission sites was locally measured up to 1 nA or 1  $\mu\text{A}$ . Field emission current processing (FECP) was performed on two samples

at 1 nA up to 5 minutes and on the other two at 1  $\mu\text{A}$  for typically 15 minutes. This strategy was chosen for the planned comparison of current with ion impact conditioning. The actual field  $E_{\text{on}}$  was calibrated for each emitter as slope of PID-regulated  $V(z)$  plot for 1 nA. Using the modified Fowler-Nordheim law [7]

$$I_{FN} = A \frac{S\beta^2 E^2}{\phi t^2(y)} \exp\left(-B \frac{\phi^{3/2} v(y)}{\beta E}\right) \quad (1)$$

the field enhancement factor  $\beta_{FN}$  and the emitting area  $S_{FN}$  can be calculated for a given work function  $\phi$  at the beginning and at the end of the FECP. For simplicity, we have taken  $\phi = 4 \text{ eV}$  (Nb),  $v(y) = t(y) = 1$ ,  $A = 154$  and  $B = 6830$  for  $E$  in MV/m and  $I_{FN}$  in A.

The surface quality of the samples was investigated in areas of 1  $\text{mm}^2$  before the FESM measurements using a commercial optical Profilometer (OP) installed on a granite plate with an active damping system in a clean (cleanroom class ISO5) laminar air flow (Fig. 1). Samples up to 20 $\times$ 20  $\text{cm}^2$  and a max. height difference of 5 cm can be measured with a lateral (vertical) resolution of 2  $\mu\text{m}$  (3 nm) by means of the spectral reflection and chromatic aberration of white light. A CCD camera is installed for fast orientation. Further zooming into a scan area of 98 $\times$ 98  $\mu\text{m}^2$  is achieved by using an AFM which can be positioned within  $\pm 2 \mu\text{m}$  of OP results with a lateral (vertical) resolution of 3 nm (1 nm). Using these results, the linear and square roughness  $R_a$  and  $R_q$  of the surfaces can be calculated and the geometric field enhancement factor  $\beta_{\text{geo}}$  of pronounced features can be estimated. Finally scanning electron microscopy (SEM) with energy dispersive x-ray analysis (EDX,  $Z > 10$ ) was applied to search for the EFE origin and foreign materials at the emission site within a correlation accuracy of  $\pm 100 \mu\text{m}$ .

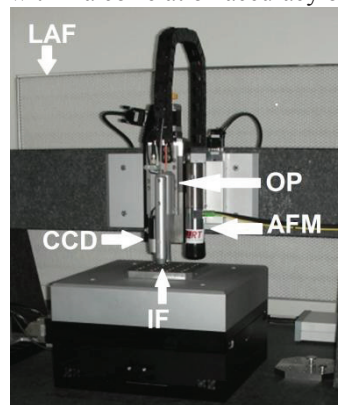


Figure 1: Measurement system for surface quality: camera (CCD), optical profilometer (OP), atomic force microscope (AFM), interferometer (IF) in front of laminar air flow (LAF).

Sample Preparation

Four round ( $\varnothing \cong 23 - 26$  mm) SC Nb discs (RRR > 250) were polished at TJNAF in two steps: 1. buffered chemical polishing (BCP) using HF, HNO<sub>3</sub> and H<sub>3</sub>PO<sub>4</sub> in the volume ratio of 1:1:2 with polishing depths of 20, 40, 80 and 120  $\mu\text{m}$  and 2. electropolishing (EP) using HF and H<sub>2</sub>SO<sub>4</sub> in a volume ratio of 1:10 with complementary depths values. The overall polishing depth is nearly constant (136 – 138  $\mu\text{m}$ ), but different  $r_p$  values (0.15 – 5.80) result for each sample (Table 1). After both steps the discs were rinsed with ultrapure water, wrapped up in soft tissues (BCP) or protected with a Teflon cap (EP) and transported to Wuppertal.

Table 1: Polishing depths for BCP and EP, total polishing depth and  $r_p$  for all samples.

sample	#1	#2	#3	#4
BCP [ $\mu\text{m}$ ]	20	40	80	120
EP [ $\mu\text{m}$ ]	116	96	58	18
$\Sigma$ [ $\mu\text{m}$ ]	136	136	138	138
$r_p$	5.80	2.40	0.73	0.15



Figure 2: SC Nb sample on holder with protection cap.

The Nb discs were glued with a conductive tape on a cathode holder and covered with a Teflon protection cap (Fig. 2). For the final cleaning of these samples and caps we used a commercial DIC system (SJ-10, CryoSnow GmbH) with a gun in laminar air flow box (cleanroom class ISO5) as shown in Fig. 3. At a propellant gas (N<sub>2</sub>) pressure of 8 bar and a liquid CO<sub>2</sub> pressure of 10 bar, it provides a flat jet (12 mm width and 3 mm height in 5 cm distance) of CO<sub>2</sub> snow particles. The samples (caps) were manually DIC cleaned under rotation (4×90°) in total for 5 (3) minutes. The protection caps were not removed until the samples faced at least high-vacuum conditions in the load-lock of the FESM, and also used for transport to other measurement systems. The samples have two marks on the edge for correlated positioning in FESM, OP and SEM.

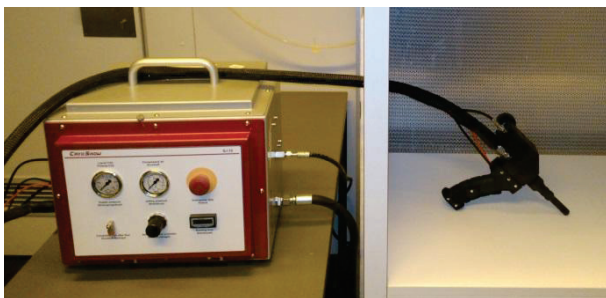


Figure 3: DIC system with control panel and gun.

RESULTS AND DISCUSSION

Surface Quality

Typical defect-free OP profiles of each sample after both polishing steps and cleaning with ionized N<sub>2</sub> (5 bar) are compared in Fig. 4. Small pits ( $\varnothing \approx 50$   $\mu\text{m}$ , height < 1  $\mu\text{m}$ ) are always present. As expected, the influence of EP on the surface quality is most pronounced for sample #1, less for sample #2 and negligible for sample #3 and #4.

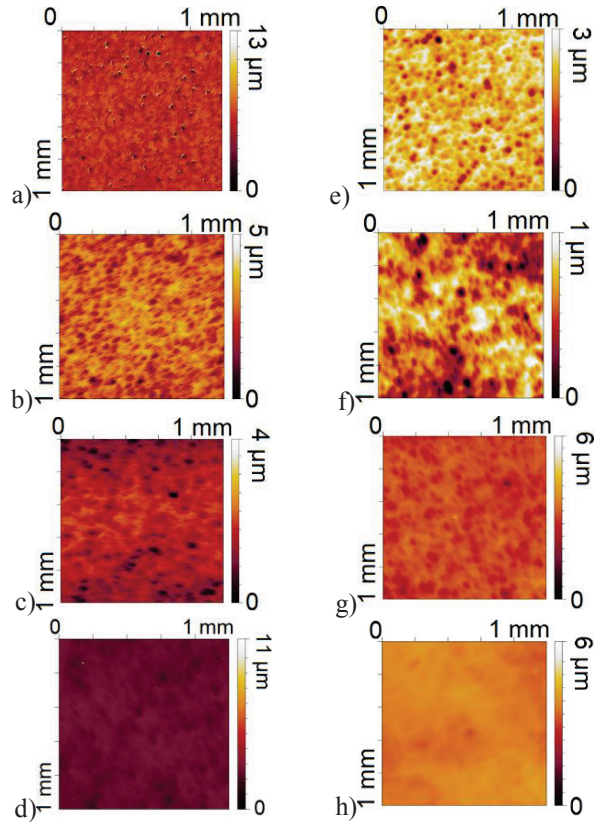


Figure 4: Surface profiles (OP) of sample #1 (a, e), #2 (b, f), #3 (c, g) and #4 (d, h) after the BCP (a – d) and after the EP (e – h). Please note the different height scales.

The mean values for  $R_a$  and  $R_q$  calculated from these profiles (Fig. 5) indicate that after BCP on SC Nb the resulting roughness is reduced up to a polishing depth of 80  $\mu\text{m}$ . BCP between 80 and 120  $\mu\text{m}$  leads to similar  $R_a$  and  $R_q$  values, i.e. more sharp features are removed. Combination of BCP with EP leads to a reduced roughness for  $r_p \geq 2.40$  (sample #1 & #2), but similar surface quality as BCP only for  $r_p \leq 0.73$ .

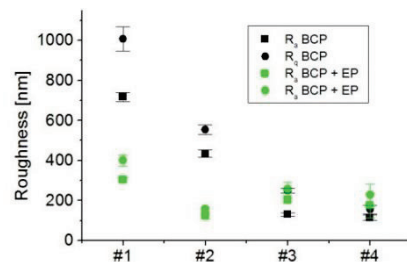


Figure 5:  $R_a$  and  $R_q$  of each sample after BCP and EP.

Despite the high average surface quality of the samples, rather few surface defects were also found on the OP profiles and further investigated with AFM. Within the limited resolution of OP and AFM profiles, maximum  $\beta_{\text{geo}}$  values up to 10 could be derived for such defects.

### EFE Statistics

Similar  $N$  values were obtained from the field maps for all samples at the same field levels, e.g.  $N = 5 - 8 \text{ cm}^{-2}$  at 200 MV/m (Fig. 6). It is remarkable that  $E_{\text{act}}$  for these DIC-cleaned SC Nb surfaces is much higher than for DIC-cleaned polycrystalline Nb [1] and for high-pressure-rinsed SC and LG [6].

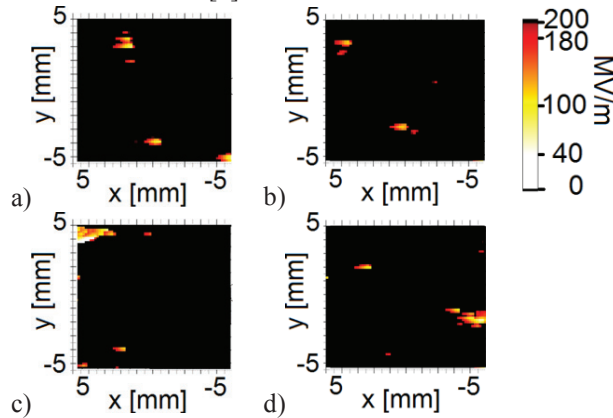


Figure 6: Field maps up to 200 MV/m of sample #1 (a), #2 (b), #3 (c) and #4 (d).

The  $E_{\text{on}}$  values (Fig. 7) resulting from locally measured  $I(V)$  curves scatter between 50 and 160 MV/m for three samples (#1, #3 and #4), while sample #2 was measured up to 240 MV/m to improve the statistics. On average the field reduction factor  $E_{\text{act}}/E_{\text{on}}$  was about  $1.5 \pm 0.5$ , but a dependency on  $r_p$  is not visible.

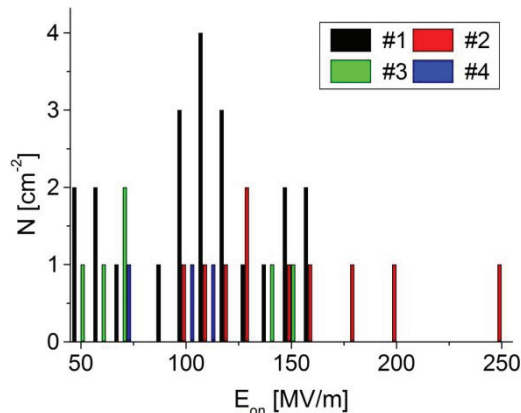


Figure 7: Histogram of locally measured  $E_{\text{on}}$ .

$N(E_{\text{act}})$  (Fig. 8) shows the typical exponential rise for all samples within the error bars. Extrapolation to  $E_{\text{act}} = 70 \text{ MV/m}$  ( $E_{\text{peak}}$  of actual ILC cavities) by using the fit function

$$\ln N(E_{\text{act}}) = a \cdot E_{\text{act}} + b \quad (2)$$

indicates, that at this field level sample #1 ( $a = 0.04013 \text{ m/MV}$ ,  $b = -6.08798$ ) would have the lowest  $N \cong 0.0377$

$\text{cm}^{-2}$ . Sample #4, however, gives  $N \cong 0.2925 \text{ cm}^{-2}$ . Accordingly, at least 1 emitter has to be expected in  $26.55$  ( $3.42$ )  $\text{cm}^2$  for maximum (minimum)  $r_p$  value. Assuming that a single cell Nb cavity has an EFE sensitive iris area of about  $50 \text{ cm}^2$ , ILC 9-cell cavities even build from EP SC Nb will still suffer from EFE. Consequently, processing of these emitters will be necessary.

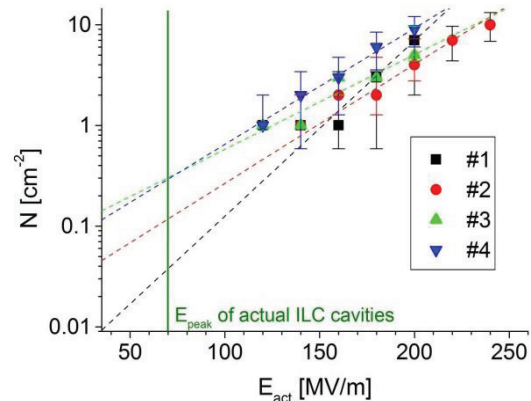


Figure 8:  $N(E_{\text{act}})$  with exponential fits (least square).

SEM investigations of the 14 strongest emission sites showed surface defects (50%), particulates (15%) and unidentified or destroyed objects. EDX in regions with particulates and destroyed objects showed always Nb and one W particulate (probably from the anode).

### Field Emitter Current Processing

The FECP up to 1 nA ( $1 \mu\text{A}$ ) were performed on 62% (38%) of the emission sites located within the field maps. The FECP up to 1 nA did not affect the emitters significantly. The example in Fig. 9 shows a slight increase of EFE by processing ( $\beta_{\text{FN}}$ :  $21 \rightarrow 20$ ,  $S_{\text{FN}}$ :  $10^{-4} \rightarrow 10^{-3} \mu\text{m}^2$ ). Some other emitters were weakened. SEM images taken in these regions showed rarely destructions (29%).

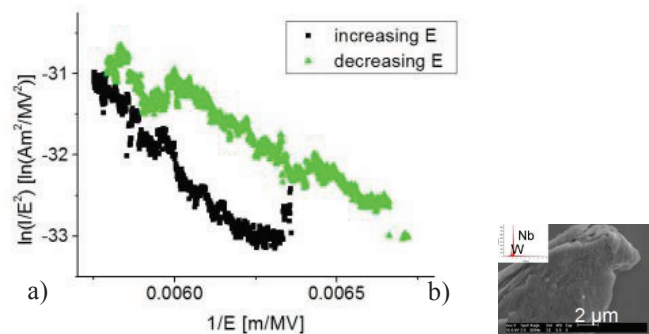


Figure 9: (a) FECP up to 1 nA on a W particulate (b).

The FECP up to  $1 \mu\text{A}$  was more often able to change the emitters significantly. The example in Fig. 10 shows the rare case of weakening at high fields ( $\beta_{\text{FN}}$ :  $63 \rightarrow 24$ ,  $S_{\text{FN}}$ :  $10^{-6} \rightarrow 10^{-2} \mu\text{m}^2$ ). However, most emitters were only stabilized by high current FECP and showed a reduced  $E_{\text{on}}$  by a factor  $\leq 2$ . SEM images taken in regions with FECP up to  $1 \mu\text{A}$  showed more often destructions (43%), which might be the origin of these activation effects.

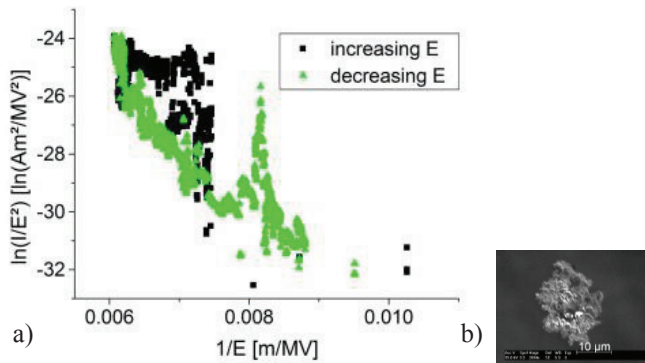


Figure 10: FN (a) FECP up to 1 μA on a surface feature (b).

Altogether the FECP of about 40 emitters reduces the scatter of their  $\beta_{FN}$  and  $S_{FN}$  values as shown in Fig. 11. With one exception the  $\beta_{FN}$  values are on average more reduced by FECP at 1 μA than at 1 nA. Unreasonable  $S_{FN}$  values, most likely caused by adsorbates effects are removed at both current levels.

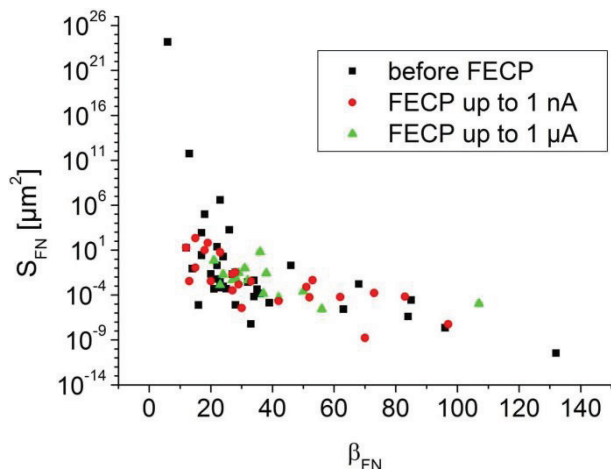


Figure 11:  $S_{FN}$  versus  $\beta_{FN}$  plot before and after FECP up to 1 nA and 1 μA.

Nevertheless the emitters cannot be completely destructed and low  $E_{on}$  down to 40 MV/m was still observed after FECP up to 1 μA (Fig. 12).

## CONCLUSIONS AND OUTLOOK

In terms of surface roughness and remaining defects, polishing of SC Nb with more EP than BCP provides the

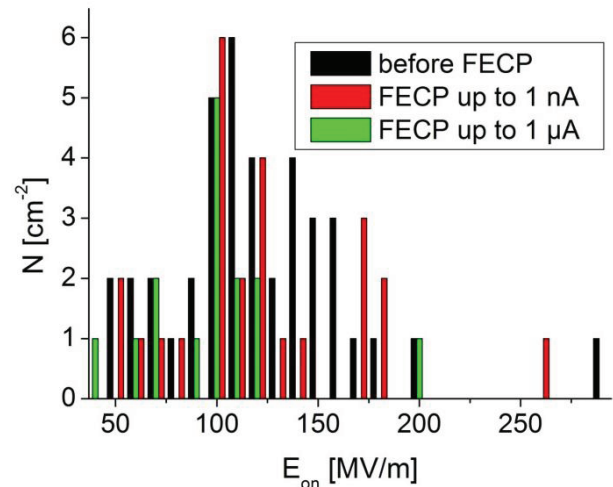


Figure 12:  $N(E_{on})$  histogram before and after the FECP.

best surface quality. For the DIC-cleaned SC samples, however, we could not observe a dependency of EFE properties on the  $r_p$  value. FECP up to 1 μA is able to weaken strong emitters, but extrapolation of  $N$  to 70 MV/m indicates that actual ILC cavities will suffer from EFE even after DIC. The measurement series should be repeated on LG or polycrystalline Nb, because the effect of  $r_p$  on the EFE might be different. Ion processing of emitters with Ar and He might be more effective than FECP.

## ACKNOWLEDGMENTS

Acknowledgements are given to Dr. A. Navitski for detailed discussions, Dr. R. Heiderhoff for access to SEM facility at FB E of University of Wuppertal, to P. Dhakal for EP at TJNAF. The work is funded by BMBF project 05H12PX6.

## REFERENCES

- [1] A. Navitski, PhD thesis, Univ. Wuppertal (2010).
- [2] A. Dangwal et al., J. Appl. Phys. 102, 044903 (2007).
- [3] Reschke et al., Phys. Rev. ST Accel. Beams 13, 071001 (2010).
- [4] ILC Technical Design Report (June 2013).
- [5] J. Knobloch, H. Padamsee, Proc. of the 8th SRF-Workshop, Padova, Italy p. 994 (1997).
- [6] See contribution TUP094, these proceedings.
- [7] R. G. Forbes, J. Vac. Sci. Technol. B 17, 526 (1999).